Available online at www.sciencedirect.com
ScienceDirect
Biochimica et Biophysica Acta 1768 (2007) 2787–2800
Biochimica et Biophysica Acta
BBA
www.elsevier.com/locate/bbamem

Interactions of the Australian tree frog antimicrobial peptides aurein 1.2, citropin 1.1 and maculatin 1.1 with lipid model membranes: Differential scanning calorimetric and Fourier transform infrared spectroscopic studies

Gordon W.J. Seto [a], Seema Marwaha [a], Daniel M. Kobewka [a], Ruthven N.A.H. Lewis [a], Frances Separovic [b], Ronald N. McElhaney [a,*]

[a] *Department of Biochemistry, University of Alberta, Edmonton, Alberta, Canada T6G 2H7*
[b] *School of Chemistry, Bio21 Institute, University of Melbourne, Melbourne VIC 3010, Australia*

Received 30 May 2007; received in revised form 6 July 2007; accepted 16 July 2007
Available online 10 August 2007

Abstract

The interactions of the antimicrobial peptides aurein 1.2, citropin 1.1 and maculatin 1.1 with dimyristoylphosphatidylcholine (DMPC), dimyristoylphosphatidylglycerol (DMPG) and dimyristoylphosphatidylethanolamine (DMPE) were studied by differential scanning calorimetry (DSC) and Fourier-transform infrared (FTIR) spectroscopy. The effects of these peptides on the thermotropic phase behavior of DMPC and DMPG are qualitatively similar and manifested by the suppression of the pretransition, and by peptide concentration-dependent decreases in the temperature, cooperativity and enthalpy of the gel/liquid–crystalline phase transition. However, at all peptide concentrations, anionic DMPG bilayers are more strongly perturbed than zwitterionic DMPC bilayers, consistent with membrane surface charge being an important aspect of the interactions of these peptides with phospholipids. However, at all peptide concentrations, the perturbation of the thermotropic phase behavior of zwitterionic DMPE bilayers is weak and discernable only when samples are exposed to high temperatures. FTIR spectroscopy indicates that these peptides are unstructured in aqueous solution and that they fold into α-helices when incorporated into lipid membranes. All three peptides undergo rapid and extensive H–D exchange when incorporated into D_2O-hydrated phospholipid bilayers, suggesting that they are located in solvent-accessible environments, most probably in the polar/apolar interfacial regions of phospholipid bilayers. The perturbation of model lipid membranes by these peptides decreases in magnitude in the order maculatin 1.1 > aurein 1.2 > citropin 1.1, whereas the capacity to inhibit *Acholeplasma laidlawii* B growth decreases in the order maculatin 1.1 > aurein 1.2 ≅ citropin 1.1. The higher efficacy of maculatin 1.1 in disrupting model and biological membranes can be rationalized by its larger size and higher net charge. However, despite its smaller size and lower net charge, aurein 1.2 is more disruptive of model lipid membranes than citropin 1.1 and exhibits comparable antimicrobial activity, probably because aurein 1.2 has a higher propensity for partitioning into phospholipid membranes.

Keywords: Lipid–peptide interaction; Antimicrobial peptide; Aurein 1.2; Citropin 1.1; Maculation 1.1; Lipid bilayer membrane; DSC; FTIR spectroscopy

Abbreviations: AMP, antimicrobial peptide; DSC, differential scanning calorimetry; FTIR, Fourier-transform infrared; PC, phosphatidylcholine; PE, phosphatidylethanolamine; PG, phosphatidylglycerol; NMR, nuclear magnetic resonance; POPC, 1-palmitoyl, 2-oleoyl phosphatidylcholine; POPG, 1-palmitoyl, 2-oleoyl phosphatidylglycerol; DMPC, dimyristoylphosphatidylcholine; DMPG, dimyristoylphosphatidylglycerol; DMPE, dimyristoylphosphatidylethanolamine; DOPE, dioleoylphosphatidylethanolamine; DOPG, dioleoylphosphatidylglycerol; HPLC, high performance liquid chromatography; MLV, multilamellar vesicles; LD_{50}, concentration required for 50% growth inhibition; MIC, minimum inhibitory concentration

* Corresponding author. Tel.: +1 780 492 2413; fax: +1 780 492 0095.
E-mail address: rmcelhan@ualberta.ca (R.N. McElhaney).

0005-2736/$ - see front matter © 2007 Elsevier B.V. All rights reserved.
doi:10.1016/j.bbamem.2007.07.018

1. Introduction

Amphibians are known to produce a number of host defense peptides which are active against a variety of microbial pathogens [1] and the skin secretions of Australian tree frogs are rich in such antimicrobial peptides (AMPs)[1] [2]. The aureins, citropins and maculatins are three families of structurally related AMPs found in the skin secretions of several species of the Australian tree frogs of the genus *Litoria*. [3–6]. Most of these peptides exhibit antibacterial activity against both Gram-positive and Gram-negative bacteria [2], and many of them also exhibit fungicidal and anticancer activity [3], specific neuronal nitric oxide synthetase inhibitory activity [2], and the capacity to inhibit infection by enveloped viruses such as HIV [7]. These AMPs generally appear to kill their microbial target cells primarily by binding to and destabilizing the lipid bilayers of their cell membranes, a fact which provides the primary impetus for studies of their interactions with lipid bilayer model and biological membranes [8].

The three best-studied Australian tree frog AMPs are aurein 1.2, citropin 1.1 and maculatin 1.1. Aurein 1.2 is a 13-amino acid peptide (GLFDIIKKIAESF-NH_2) produced by the Australian green and golden bell frog *Litoria aureus* and by the related Australian southern bell frog *Litoria raniformis* [3]. This peptide is cationic at physiological pH with a net charge +1. The 16-amino acid peptide citropin 1.1 (GLFDVIKKVASVIGGL-NH_2) is found in the skin secretions of the Australian tree frog *Litoria citropa* [4,5]. This peptide is also cationic at physiological pH but with a net charge of +2. Maculatin 1.1 (GLFGVLAK-VAAHVVPAIAEHF-NH_2) is produced by the Australian tree frog *Litoria genimaculata* [5]. This peptide is also cationic but is larger (21 amino acid residues) with a net charge of +3 at physiological pH. Notwithstanding the differences in the primary structures of these three tree frog AMPs, there are a number of common structural features which appear to be functionally important. Indeed, they are all C-amidated linear polypeptides with charged N-termini composed of the sequence Gly–Leu–Phe, and one or more cationic residues located 7–8 residues from their N-termini, features which all appear to be essential for the maximal expression of their antibacterial activities [2]. In aqueous solution, these peptides adopt primarily unstructured random coil conformations but readily fold into α-helical structures in membrane-mimetic environments [3–5,9]. As illustrated in Fig. 1, they form amphipathic helices in which the polar and charged amino acids are linearly clustered on one face of the helix and the nonpolar amino acid residues clustered on the other face. However, when bound to membranes or dissolved in membrane-mimetic solvents, aurein 1.2 and citropin 1.1 both fold into single continuous α-helical structures, whereas the longer peptide maculatin 1.1 forms two distinct α-helical segments [5,10,11] separated by a so-called flexible hinge region [5]. The hinge region of maculatin 1.1 arises from the helix-disrupting properties of the Pro-15 residue, the presence of which is required for maximum antibacterial activity [10,11].

Unlike several other families of helix-forming AMPS [see 12,13], there have been relatively few studies of the interactions of these three Australian tree frog AMPs with lipid model membranes (see [8]). Monolayer studies of citropin 1.1 and maculatin 1.1 alone have established that both of these peptides are surface active. Moreover, when peptide was introduced into the aqueous subphase under monolayer films of the zwitterionic phospholipid POPC, citropin 1.1 and maculatin 1.1 appeared to form separate domains, whereas with films of the anionic phospholipid POPG, the peptide and lipid seemed to form a single phase, perhaps due to the favorable electrostatic interactions between the cationic peptide and the anionic POPG molecules [14]. Solid-state ^2H and ^{31}P-NMR studies [15,16] with bilayers of the zwitterionic phospholipid DMPC were also performed with each of these peptides, which were found to decrease the order and increase the mobility of both the DMPC polar headgroups and hydrocarbon chains. However, the interactions of these peptides with DMPC bilayers seem largely localized to the polar headgroup and glycerol backbone regions of the host phospholipid molecules. Moreover, the bilayer structure is preserved even at high peptide concentrations and the peptide molecules themselves appear highly mobile. However, other ^{31}P-NMR spectroscopic studies have shown that the incorporation of aurein 1.2 into mixed DOPE:DOPG membranes may actually promote the formation of inverted nonlamellar phases [9]. FTIR spectroscopic studies of the interaction of maculatin 1.1 with DMPC and DMPG bilayers showed a marked preference of this peptide for binding to the anionic phospholipid, in that about 70% of the amino acid residues underwent amide H–D exchange when added to DMPC vesicles, whereas only 5% did so when added to DMPG vesicles [17]. Finally, solid-state ^{31}P-NMR spectroscopic studies of the interactions of maculatin 1.1 with live Gram-positive bacteria indicate that the bacterial membrane were lysed and the phospholipid bilayers were converted to small, micelle-like structures [18], in contrast to the NMR results with DMPC model membranes discussed above [11,14].

DSC is a powerful, nonperturbing thermodynamic technique which has proven very useful for studies of lipid–protein interactions in model and biological membranes in general (see [19–21]) and for the study of the interactions of AMPs with lipid bilayer model membranes in particular (see [22,23]). In order to study the interactions of the frog AMPs aurein 1.2, citropin 1.1 and maculatin 1.1 with various phospholipid bilayer membranes, we have utilized DSC to study the effect of these peptides on the thermotropic phase behavior of the major phospholipid classes of bacterial and animal cells. Specifically, we have studied the effect of various concentrations of these three peptides on the pretransition and main transition of zwitterionic DMPC and anionic DMPG, and on the main phase transition of zwitterionic DMPE bilayer membranes. Since PCs are virtually absent in bacterial membranes but are generally the most abundant phospholipid class in eukaryotic plasma membranes, DMPC bilayers can serve as a model for the surface membrane of the cells of higher animals, especially as PCs are typically localized primarily in the outer monolayer of the lipid bilayer of such membranes. Similarly, PGs are absent from eukaryotic

[1] See abbreviations.

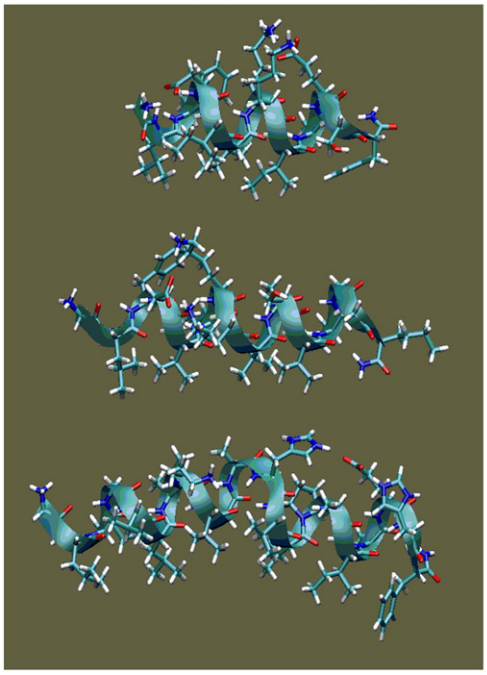

Fig. 1. Molecular models of the structures expected of aurein 1.2, citropin 1.1 and maculatin 1.1 bound to lipid membranes. The coordinates used to draw these models were obtained from previously published NMR-determined solution structures of these peptides in membrane-mimetic media [4,5,9].

plasma membranes, but are ubiquitous and often abundant in prokaryotic surface membranes. Moreover, PEs are major constituents of all eukaryotic plasma membranes and are also abundant in most Gram-positive bacteria and in members of the Gram-positive *Bacillus* bacteria as well, although PEs are usually enriched in the inner monolayer of the lipid bilayer of eukaryotic plasma membranes. Thus DMPE bilayers can serve as a relevant model for the lipid bilayers of both animal and bacterial membranes. We have also utilized FTIR spectroscopy to study the conformation of these antimicrobial peptides as dry films or when dissolved in aqueous buffer, as well as when bound to DMPC, DMPE and DMPG bilayers in the gel and liquid–crystalline phases, and to investigate the effect of these peptides on the organization of the host phospholipid bilayer. The results of these studies were correlated with the intrinsic capacities of these peptides to disrupt the lipid bilayer of a cell membrane as assayed by their capacity to inhibit the growth of the cell wall-less mollicute *Acholeplasma laidlawii* B.

2. Materials and methods

DMPC, DMPE and DMPG were purchased from Avanti Polar Lipids (Alabaster, AL, USA) and were used without further purification. Aurein 1.2, citropin 1.1 and maculatin 1.1 were chemically synthesized (Mimotopes, Melbourne, Australia and the Alberta Peptide Institute, Edmonton, Alberta, Canada) by solid-phase techniques using Fmoc chemistry, and were shown to be >95% pure by HPLC and mass spectrometry [24,25].

Samples were prepared for DSC as follows. Lipid and peptide were codissolved in methanol to attain the desired lipid-to-peptide ratio and the solvent was removed with a stream of nitrogen, leaving a thin film on the sides of a clean glass test tube. This film was subsequently dried *in vacuo* overnight to ensure removal of the last traces of solvent. Samples containing ~1.0 mg of lipid were then hydrated by placing some wet cotton wool into the tube (without contacting the lipid/peptide film) and allowing the sample to absorb water from the water vapour-saturated air by warming the sample to temperatures well above the expected gel/liquid–crystalline phase transition temperature of the lipid [26]. Subsequently, the cotton wool was removed and the hydrated sample quickly dispersed by vigorous vortexing with a known volume (typically 0.5–2.0 ml) of a prewarmed buffer composed of 50 mM Tris, 150 mM NaCl, 1 mM NaN3, pH 7.4, at temperatures some 10–15 °C above the lipid gel/liquid–crystalline phase transition temperature. The variation in the dispersal volume utilized was done primarily to increase the sample size of the peptide-rich samples so that the broader thermograms exhibited by these samples could be more accurately recorded. DSC thermograms were obtained from 0.324 ml samples with a high-sensitivity Nano DSC instrument (Calorimetry Sciences Corporation, Lindon, UT, USA) operating at heating and cooling rates of 10 °C/h. The data were analyzed and plotted with the Origin software package (OriginLab Corporation, Northampton, MA, USA). In cases where the DSC thermograms appeared to be a summation of overlapping components, the midpoint temperatures, areas and widths of the components were estimated with Origin nonlinear least squares curve- and peak-fitting procedures, and a custom-coded function based on the assumption that the observed thermogram was a linear combination of components, each of which approximates a reversible, two-state transition at thermodynamic equilibrium.

FTIR spectroscopy was performed on dried films and on aqueous solutions of these frog AMPs, and on fully hydrated peptide–lipid dispersions. Typically, dried films of the peptide were cast from methanolic solution onto a solid support, typically one of the CaF_2 windows of the demountable liquid cell described below, followed by removal of the solvent. The hydrated peptide and lipid:peptide samples were prepared for FTIR spectroscopy by dissolving the peptide or by co-dissolving lipid and peptide in methanol at a lipid-to-peptide ratio of 30:1 (mol/mol). After removal of the solvent and drying of the film, samples containing peptide, or peptide and 2–3 mg of lipid, were hydrated by vigorous mixing with 75 μL of a D_2O-based buffer (50 mM Tris, 150 mM NaCl, 1 mM NaN_3, pH 7.4). The dispersion obtained was then squeezed between the CaF_2 windows of a heatable, demountable liquid cell (NSG Precision Cells, Farmingdale, NY) equipped with a 25-μm Teflon spacer. Once mounted in the sample holder of the spectrometer, the sample temperature could be varied between 0 and 90 °C by an external, computer-controlled water bath. FTIR spectra were acquired as a function of temperature with a Digilab FTS-40 Fourier-transform spectrometer (Bio-Rad, Digilab Division, Cambridge, MA, USA) using data acquisition parameters similar to those described by Mantsch et al. [27]. With hydrated lipid:peptide mixtures, the experiment typically

involves a sequential series of 2 °C temperature ramps punctuated by a 20 min inter-ramp delay for thermal equilibration, and was equivalent to a scanning rate of 4 °C/h. Spectra were analyzed with software supplied by the instrument manufacturers and computer programs obtained from the National Research Council of Canada.

The cell wall-less mollicute *A. laidlawii* B was cultured in chloroform-extracted BSA-free media and cell growth was monitored turbidometrically [28]. The effect of these antimicrobial peptides on cell growth was monitored as a function of time and peptide concentration after the addition these peptides to the culture medium just prior to a 10% (by volume) inoculation with cells in the mid-log phase of growth. Cell growth was examined in media containing up to 10 μM peptide and is expressed relative to the maximum growth obtained in the absence of peptide. Where feasible, the growth inhibitory properties of the peptides were expressed in terms of apparent LD_{50} values as described previously [29].

3. Results

3.1. Differential scanning calorimetry

DSC heating thermograms, illustrating the effect of the incorporation of increasing quantities of the peptides aurein 1.2, citropin 1.1 and maculatin 1.1 on the thermotropic phase behavior of MLVs composed of the lower melting zwitterionic phospholipid DMPC, are presented in Fig. 2. In the absence of peptide, DMPC MLVs which have not been extensively annealed at lower temperatures exhibit two endothermic events on heating, a weakly energetic pretransition near 14 °C and a strongly energetic main phase transition near 24 °C. The pretransition arises from the conversion of a lamellar gel phase with tilted hydrocarbon chains (the L_{β}' phase) to a rippled gel phase also with tilted hydrocarbon chains (the P_{β}' phase), while the main or hydrocarbon chain-melting phase transition arises from the conversion of the P_{β}' to the lamellar liquid–crystalline (L_{α}) phase. The reader is referred to Lewis et al. [30] for a more detailed description of the thermotropic phase behavior of MLVs of DMPC and of other members of the homologous series of linear saturated PCs. Note that the cooling exotherms

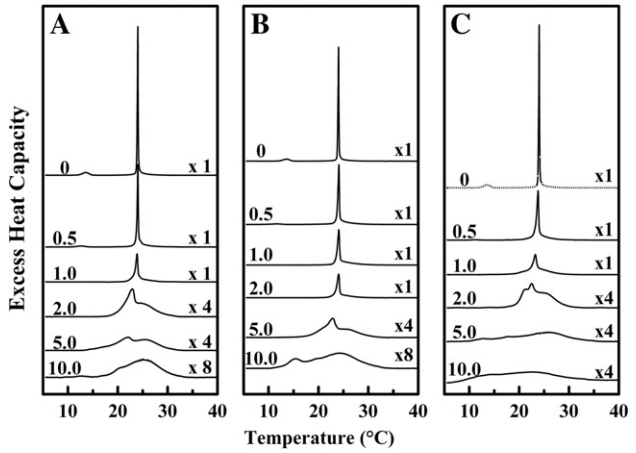

Fig. 2. DSC heating thermograms illustrating the effects of aurein 1.2 (A), citropin 1.1 (B) and maculatin 1.1 (C) on the thermotropic phase behavior of aqueous dispersions of DMPC. The thermograms shown were normalized for lipid sample mass and were acquired at the peptide concentrations (mol%) indicated on the left of each thermogram. The labels to the left of each thermogram indicate the relative Y-scaling factors used for plotting.

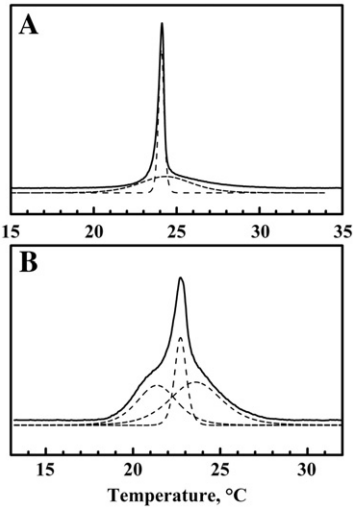

Fig. 3. Illustration of the resolvable components found in the DSC thermograms exhibited by lipid bilayers composed of peptide-poor (A) and peptide-rich (B) mixtures of aurein 1.2, citropin 1.1 and maculatin 1 with DMPC and DMPG.

observed with DMPC and with its mixtures with all three peptides (not shown here) exhibit near mirror image symmetry relative to the heating endotherms, indicating that the major thermotropic events were recorded under conditions very close to thermodynamic equilibrium.

As illustrated in Fig. 2, the incorporation of these peptides into DMPC MLVs significantly alters their thermotropic phase behavior. Specifically, the presence of small amounts of these peptides (DMPC:peptide ratio 200:1) reduces the temperature and enthalpy of the pretransition and abolishes the pretransition entirely at higher peptide concentrations. Moreover, small quantities of these peptides initially induce a two-component main phase transition, composed of a lower temperature, more cooperative endotherm superimposed over a higher temperature, less cooperative (broader) endotherm (see Fig. 3A). As peptide concentration increases, the temperature, (Fig. 4A), enthalpy (Fig. 4B) and cooperativity of the sharp component all decrease, whereas the temperature and enthalpy of the broad component initially increase slightly, (Fig. 4B). Further increases in peptide concentration also result in the progressive decline and eventual elimination of the sharp component and the formation of a third, lower temperature broad component (see Fig. 3B) which grows progressively in intensity with increasing peptide concentration (see Fig. 4B). Finally, with all of these peptides, the total enthalpy of the main phase transition (the sum of the areas of all endothermic components) initially decreases fairly rapidly with increasing peptide concentration and then declines less rapidly at higher peptide concentrations (see Fig. 5). In analogy to our previous DSC studies of binary mixtures of α-helical transmembrane peptides [31,32] and of the AMP gramicidin S [22] with various phospholipids, we assign the sharp and broad components of the DSC endotherm to the chain-melting phase transition of peptide-poor and peptide-rich phospholipid domains, respectively. This interpretation of these DSC results is supported our FTIR spectroscopic studies (see below).

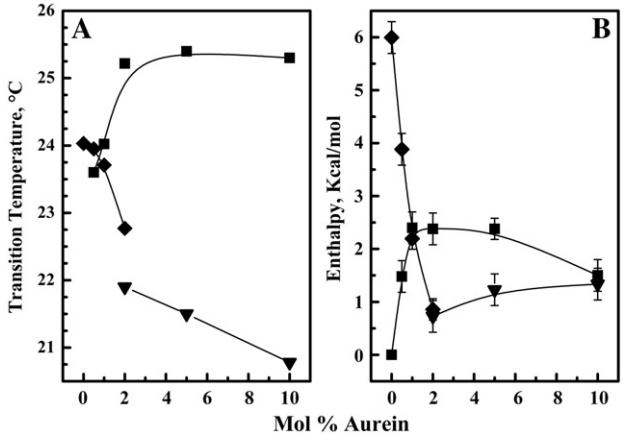

Fig. 4. Illustration of the general effect of peptide concentration on the temperature (A) and enthalpy (B) of the components resolved in the DSC thermograms exhibited by mixtures of the aurein 1.2, citropin 1.1 and maculatin 1.1 with DMPC and DMPG. The datasets shown were derived from the thermograms exhibited by aurein 1.2-containing DMPC mixtures, and represent the properties of the sharp component of DSC thermogram (–◆–), the higher-temperature broad component initially observed at low-peptide concentrations (–■–), and the lower-temperature broad component observed at very high peptide concentrations (–▼–).

Although the general effects of these three peptides on the thermotropic phase behavior of DMPC MLVs are qualitatively similar, close inspection of the data indicates the effects of each peptide differ markedly in magnitude. With the citropin 1.1-containing MLVs, the sharp component of the DSC thermogram persists to higher peptide concentrations than observed with aurein 1.2 and maculatin 1.1, and the peptide concentration-induced diminution in its temperature and enthalpy is smaller than observed with the latter two peptides (Fig. 5). Also, at comparable peptide concentrations, the broad components observed in the citropin 1.1-containing preparations are not as prominent as those observed in the corresponding aurein 1.2- and maculatin 1.1-containing MLVs (Fig. 2), and the peptide-induced decline in the overall transition enthalpy is less pronounced than occurs with the other those peptides (Fig. 5B). In contrast, maculatin 1.1 produces a greater reduction in the temperature (Fig. 5A), enthalpy (Fig. 5B) and cooperativity of the sharp component, which is abolished at lower peptide concentrations, and the reduction in the overall enthalpy of the phase transition (Fig. 5) is greater than observed with either aurein 1.2 or citropin 1.1. Thus, at comparable peptide concentrations, the relative magnitude of the perturbation of the thermotropic phase behavior of DMPC MLVs decreases in the order maculatin 1.1 > aurein 1.2 > citropin 1.1.

DSC heating scans illustrating the effect of aurein 1.2, citropin 1.1 and maculatin 1.1 on the thermotropic phase behavior of DMPG MLVs are presented in Fig. 6. As observed with DMPC, the main cooling exotherms exhibited by pure lipid and by its mixtures with all three peptides (not shown here) also exhibit near mirror image symmetry relative to the baseline, indicating that the major thermotropic events were recorded under conditions approaching thermodynamic equilibrium. Aqueous dispersions of DMPG which have not been extensively annealed at low temperatures, also exhibit a weakly energetic transition near 12 °C and a more energetic phase transition near 24 °C. As with DMPC bilayers, the pretransition arises from the conversion of the L_{β}' gel to the P_{β}' gel phase and the main transition or chain-melting phase transition from the conversion of the P_{β}' to the L_{α} phase. A subtransition is not observed under these conditions since these DMPG MLVs were not annealed at low temperatures. For a more detailed discussion of the thermotropic phase behavior of DMPG and other members of the homologous series of linear saturated PGs, see Zhang et al. [33].

It is clear that these peptides have a major effect on their thermotropic phase behavior of DMPG MLVs, and that there are a number of qualitative similarities between their effects on DMPC and DMPG bilayers (see Figs. 2 and 6). Thus, as

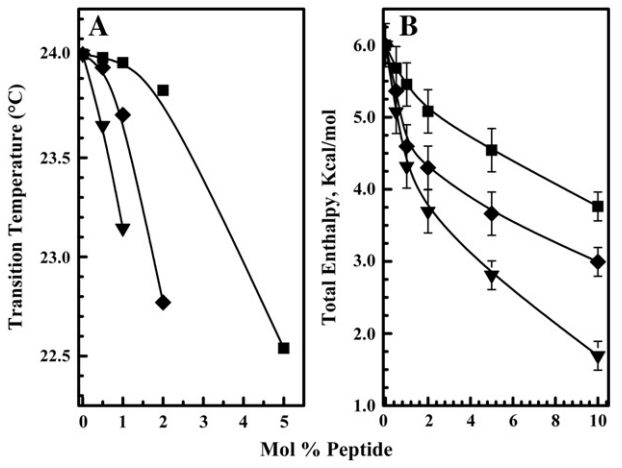

Fig. 5. Effect of peptide concentration on the properties of the DSC thermograms exhibited by mixtures of DMPC with aurein 1.2 (–◆–), citropin 1.1 (–■–) and maculatin 1.1 (–▼–). The data shown illustrate the effects of peptide concentration on (A) the transition temperatures of the sharp components in the DSC thermograms, (B) the total enthalpy of all of the components resolved.

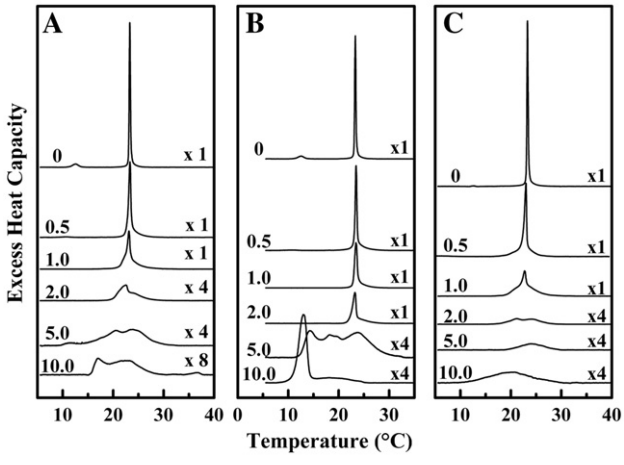

Fig. 6. DSC heating thermograms illustrating the effects of aurein 1.2 (A), citropin 1.1 (B) and maculatin 1.1 (C) on the thermotropic phase behavior of aqueous dispersions of DMPG. The data shown were normalized for lipid sample mass and acquired at the peptide concentrations (mol%) indicated on the left of each thermogram. The labels to the left of each thermogram indicate the relative Y-scaling factors used for plotting.

observed with DMPC, the incorporation of small quantities of these peptides completely abolishes the pretransition of DMPG dispersions. Moreover, the presence of increasing quantities of these peptides initially induces a two-component main phase transition, consisting of a lower temperature, more cooperative endotherm superimposed over a high temperature, less cooperative endotherm. The temperature (Fig. 7A), enthalpy (Fig. 7B) and cooperativity of the sharp component again decrease as peptide concentration increases, while the temperature of the broad component increases slightly but its enthalpy and cooperativity decrease considerably. At higher peptide concentrations, very broad, multicomponent DSC endotherms are also observed and the total enthalpy of the main phase transition (the sum of all the components observed) initially decreases markedly and then declines less rapidly as peptide concentrations increase. Notwithstanding these overall similarities, however, a comparison of the data shown in Figs. 5 and 7 clearly indicates that with each of these cationic antimicrobial peptides, the perturbation of the thermotropic phase behavior of anionic DMPG bilayers is significantly greater than observed with zwitterionic DMPC bilayers at comparable peptide concentrations, underscoring the importance of membrane surface charge in the interactions of these peptides with lipid membranes.

Although there are qualitative similarities between the effects of these three peptides on the thermotropic phase behavior of DMPG, it is also clear that, as observed with DMPC, the effects of each peptide differ substantially in magnitude. Thus, with the citropin 1.1-containing DMPG mixtures, the midpoint temperature of the sharp component of the DSC thermogram actually initially increases slightly relative to pure DMPG and then decreases with increasing peptide concentration (Fig. 7A). However, the peptide-induced decrease in the temperature (Fig. 7A), cooperativity and enthalpy (Fig. 7B) of this component is less than observed with either aurein 1.2 and maculatin 1.1, and, as observed with the DMPC system, the sharp component persists to higher concentrations than observed with the other two peptides. With the citropin 1.1-containing DMPG MLVs, broad, multi-component endotherms tend to predominate at higher peptide concentrations than observed with either aurein 1.2 or maculatin 1.1 (see Fig. 6), and the broad, lower-temperature endotherm which emerges at high peptide concentrations grows more rapidly as a function of peptide concentration than observed with either aurein 1.2 or maculatin 1.1 (see Fig. 6). Most probably, this aspect of the behavior of citropin 1.1-rich DMPG mixtures is reflected by the increase in their total enthalpy observed at very high peptide concentrations (see Fig. 7B). In contrast, the effect of maculatin 1.1 incorporation on the thermotropic phase behavior of DMPG MLVs is much more similar to that of aurein 1.2 (see Fig. 6). However, the decrease in the temperature (Fig. 7A) and enthalpy of the sharp and broad endothermic components, and of the total overall transition enthalpy (Fig. 7B), is greater with maculatin 1.1, indicating that it is more perturbing of the organization of DMPG bilayers than aurein 1.2. Thus, as observed with DMPC bilayers, the extent of perturbation of the organization of DMPG bilayers by the incorporation of these peptides also decreases in the order maculatin 1.1 > aurein 1.2 > citropin 1.1. The possible basis of these observations are explored in Discussion.

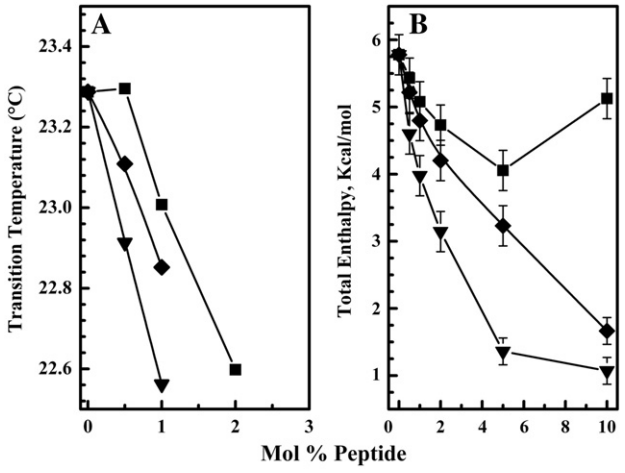

Fig. 7. Effect of peptide concentration on the properties of the DSC thermograms exhibited by mixtures of DMPG with aurein 1.2 (–◆–), citropin 1.1 (–■–) and maculatin 1.1 (–▼–). The data shown illustrate the effects of peptide concentration on (A) the transition temperatures of the sharp components in the DSC thermograms, (B) the total enthalpy of all of the components resolved.

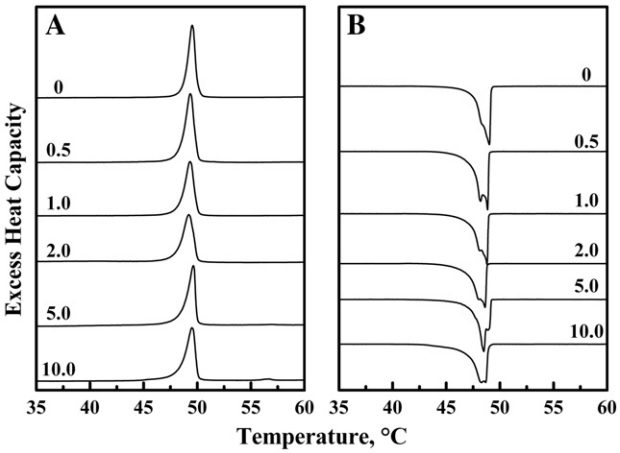

Fig. 8. DSC heating (A) and cooling (B) thermograms illustrating the effects of aurein 1.2 on the thermotropic phase behavior of aqueous dispersions of DMPE. The thermograms shown were acquired at the peptide concentrations (mol%) indicated, normalized for lipid sample mass and plotted on the same scale.

DSC heating and cooling thermograms illustrating the effects of aurein 1.2 on the thermotropic phase behavior of aqueous dispersions of the zwitterionic phospholipid DMPE are presented in Fig. 8. In the absence of peptide, DMPE MLVs which have not been incubated extensively at low temperatures exhibit a single, relatively energetic L_β/L_α phase transition near 50 °C on heating (see [34] for a complete description of the thermotropic phase behavior of DMPE and other members of the homologous series of linear saturated PEs). Upon cooling, DMPE exhibits an asymmetric multi-component exotherm, the temperatures range of which may extend to some 2 °C below that of the corresponding heating scan (Fig. 8B). This behavior differs markedly from that observed with PC and PG bilayers [34], but is commonly observed with PE bilayers and has been

ascribed to inhomogeneity in the domain structure of the liquid–crystalline state [35]. When aurein 1.2 is incorporated into DMPE vesicles, essentially no effect on the heating endotherms of the gel/liquid–crystalline phase transition is observed, even at high peptide concentrations (Fig. 8A). However, if these MLVs are heated to temperatures well above their gel/liquid–crystalline phase transition temperature, then increasing quantities of peptide modestly reduce the temperature, enthalpy and cooperativity and change the multicomponent structure of the main phase transition upon subsequent cooling (Fig. 8B). Similar results were observed with citropin 1.1 and maculatin 1.1 (data not presented), and as with DMPC and DMPG MLVs, the relative perturbation of the thermotropic phase behavior of DMPE MLVs, although modest, also decreased in the general order maculatin 1.1 > aurein 1.2 > citropin 1.1. These findings indicate that the presence of any of these three peptides produces a much smaller reorganization of DMPE than of DMPC and especially DMPG bilayers, even after maximizing peptide–DMPE interactions by exposure to high temperatures and by multiple cycling through the gel/liquid–crystalline phase transition. The fact that significant peptide-induced perturbation of the thermotropic behavior of this lipid is observed only after samples are heated to temperatures well above the gel/liquid–crystalline phase transition temperature of the lipid implies that interactions of these peptides with DMPE can be initiated only in rather fluid bilayers. In marked contrast to DMPE MLVs, peptide interactions with DMPC and DMPG MLVs can be initiated at temperatures near to or even below that of the lipid gel/liquid–crystalline phase transition (see Figs. 2 and 7).

3.2. Fourier-transform infrared spectroscopy

FTIR spectroscopy was used to monitor the conformation of these antimicrobial peptides in the dry state, when dissolved in water, and when bound to phospholipid bilayers, and also to study the effects of these peptides on the thermotropic phase behavior and organization of the host lipid membrane. Specifically, information about the conformation of these peptides can be obtained from the frequencies of the amide I and amide II absorption bands, which arise predominantly from the stretching vibrations of the amide carbonyl groups and the N–H bending vibrations of the amide protons, respectively [36]. Also, because of its sensitivity to amide H–D exchange, the intensity of the amide II band can be used to study the exchangeability of the peptide amide backbone protons and thus to provide information about the overall accessibility of the peptide amide backbone to the solvent [37,38]. Finally, the physical state and organization of the phospholipid bilayer can be evaluated by an examination of the CH_2 stretching bands, which are sensitive to the degree of rotational isomeric disorder of the lipid hydrocarbon chains, the ester carbonyl stretching band, which is sensitive to the degree of hydration and hydrogen bonding interactions in the membrane polar/apolar interfacial region, and the O–P–O asymmetric stretching band, which is also sensitive to the polarity and degree of hydration of the phosphate moiety of the phospholipid polar headgroup [39,40]. However, in these studies, the presence of these frog peptides does not seem to produce significant changes in the hydration or polarity of either the phospholipid carbonyl or phosphate groups. Thus, the only spectroscopic features presented in detail here are the amide I and II bands of the peptides and the CH_2 symmetric stretching band of the phospholipid hydrocarbon chains.

Illustrated in Fig. 9 are the amide I and C═O stretching regions of the FTIR spectra exhibited by methanol-dried and D_2O-hydrated samples of aurein 1.2 in the presence and absence of DMPC (DMPC/peptide molar ratio 30:1, corresponding to a peptide concentration of 3.3 mol%). The data shown therein are similar to those obtained with samples of citropin 1.1 and maculatin 1.1 under comparable conditions. When cast from methanolic solution, all three peptides exhibit relatively sharp amide I bands with maxima near 1658–1660 cm^{-1} and amide II bands centered near 1540–1543 cm^{-1} (see Fig. 9A). The properties of these bands are consistent with the predominance of α-helical peptide conformations under such conditions [36]. Upon hydration of these films with D_2O-based buffers, these peptides all exhibit broad, low-intensity amide I band contours centered near 1640–1660 cm^{-1} (see Fig. 9B), consistent with these peptides being predominantly unstructured in aqueous solution [36]. Also, the amide II band is completely abolished under such conditions (see Fig. 9B), as would be expected of a very flexible peptide in which all exchangeable amide protons can be readily exchanged. Fig. 9C also shows that dry, peptide-containing lipid films cast from methanolic solution exhibit sharp amide I and amide II bands with maxima near 1658–1660 cm^{-1} and 1540–1543 cm^{-1}, respectively, along with an absorption band near 1735 cm^{-1} arising from the stretching vibrations of the lipid ester carbonyl groups. However, the amide I and amide II bands observed in the lipid–peptide films are narrower than those observed with the lipid-free peptide films, consistent with the predominance of peptide α-helices with a greater degree of homogeneity of peptide conformation

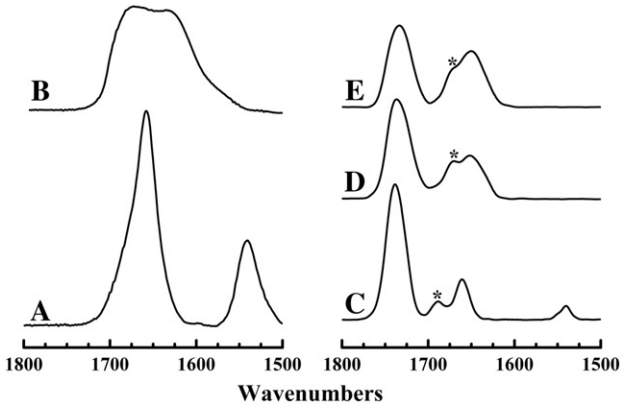

Fig. 9. Amide 1 and C═O stretching regions of the infrared spectra exhibited by (A) dry film of aurein 1.2 (cast from methanolic solution), (B) aurein 1.2 dissolved in D_2O-based buffer, (C) dry film of DMPC:aurein 1.2 mixture (lipid:peptide = 30:1, film cast from methanolic solution), (D) D_2O-hydrated DMPC:aurein 1.2 mixture (lipid:peptide = 30:1, T = 4 °C), (E) D_2O-hydrated DMPC:aurein 1.2 mixture (lipid:peptide = 30:1, T = 50 °C). The peaks marked with the asterisks arise from trifluoroacetate counterions which co-purify with the peptide during the synthesis.

when these peptides are associated with lipid. Upon hydration of the lipid–peptide films with D_2O-based buffer, some broadening of the amide I band occurs, indicating that the mobility and/or conformational flexibility of the lipid-associated peptide increases upon hydration. However, the peptide amide I band maxima also shift to frequencies near 1646–1650 cm^{-1} upon addition of D_2O and the amide II band is quickly (<5 min) abolished (see Fig. 9D and E). Also, once the sample is fully hydrated, the contours of the amide I band remain essentially insensitive to changes in both temperature and the phase state of the lipid (see Fig. 9D and E). This pattern of behavior is observed with each peptide in all of the phospholipid systems examined. The persistence of relatively sharp amide I bands, along with the downward shift in the amide I band maxima and the disappearance of the amide II band upon hydration with D_2O, are consistent with the predominance of lipid-associated α-helical peptide structures for which complete H–D exchange of backbone amide protons has occurred [36]. The fact that essentially complete amide H–D readily occurs upon D_2O hydration of dry lipid–peptide films suggests that the lipid-associated peptides are located in an environment which is accessible to the solvent and/or in an environment conducive to a rapid exchange between lipid-associated peptide α-helices and unstructured peptide molecules in the bulk solvent phase. The latter possibility is supported by the observed hydration-induced broadening of the amide I band (see Fig. 9C–E). However, it should be noted that the fast and extensive H–D exchange upon D_2O hydration of lipid:peptide films reported here differs markedly from the results of previously published FTIR spectroscopic studies, where only partial H–D exchange was observed over a much longer time period (see [17]). Most probably, the difference between the two sets of results reflects the fact that this study was performed in excess liquid D_2O whereas the previous study was performed under conditions of more limiting sample hydration.

The effect of the incorporation of these antimicrobial peptides on the chain-melting phase transition and the organization of the gel and liquid–crystalline states of the host phospholipid bilayer was also probed by an examination of the frequency of the hydrocarbon chain CH_2 symmetric stretching band as a function of temperature. As exemplified by our observations of the peptide-free and aurein 1.2-containing DMPC, DMPE and DMPG vesicles (see Fig. 10), the presence of each of these antimicrobial peptides broadens the overall gel/liquid–crystalline phase transition of the host phospholipid bilayer, although this broadening is much more pronounced in DMPC and DMPG as compared to DMPE bilayers, in agreement with the DSC results. Moreover, the incorporation of these peptides also lowers the midpoint temperature of the DMPC and DMPG vesicles, but not of the DMPE vesicles, again in agreement with the DSC findings. From the upward shift in the CH_2 symmetric stretching band frequency, it also appears that the presence of these peptides disorders the hydrocarbon chains slightly in the gel phase and more markedly in the liquid–crystalline phases of all the phospholipid vesicles studied, although this effect is again more pronounced with DMPC and DMPG than with DMPE bilayers. However, when the effects of the other peptides

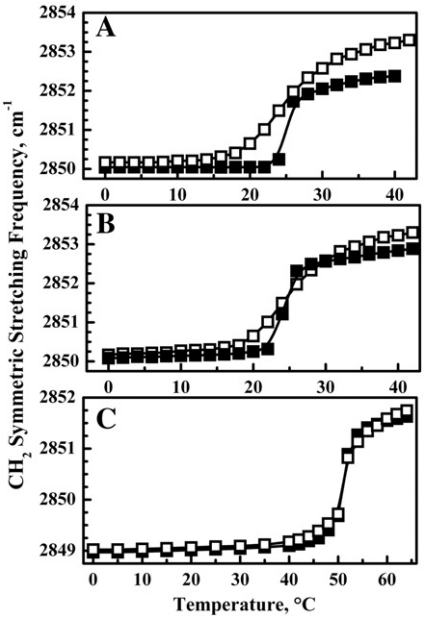

Fig. 10. Temperature-dependent changes in the frequency of the CH_2 symmetric stretching band observed in the FTIR spectra exhibited by peptide-free (–■–) and peptide-containing (–□–) phospholipid bilayers. Data are presented for: (A) DMPC:aurein 1.2 (30:1). (B) DMPG:aurein 1.2 (30:1). (C) DMPE:aurein 1.2 (30:1).

on the organization of DMPC and DMPG bilayers were compared, maculatin 1.1 seemed to have the greatest effect in disordering the gel phase than the either aurein 1.2 or citropin 1.1, although citropin 1.1 had the greatest disordering effect in the liquid–crystalline state. However, in all cases the magnitude of these hydrocarbon chain-disordering effects are relatively small in the gel state, although considerably larger in the liquid–crystalline state of DMPG and particularly of DMPC bilayer membranes.

Finally, in order to examine the structural basis of some of the broad thermotropic events observed in peptide-rich samples of DMPC and DMPG, the frequencies of the peptide amide I band and the lipid CH_2 symmetric stretching band were plotted as a function of temperature and overlaid on the DSC thermograms exhibited by mixtures of all three peptides with these phospholipids. The DMPG-based data presented in Fig. 11 typify our observations of both DMPC- and DMPG MLVs at high concentrations of these peptides. As exemplified by the data obtained in our studies of the citropin 1.1-rich DMPG samples (see Fig. 11B), the frequency of the amide I bands of these peptides changes very little with temperature, indicating that the α-helical conformation of the peptide was little affected by increases in temperature generally, or by the gel/liquid–crystalline phase transition of the host phospholipid bilayer in particular. Also, the peptide-broadened gel/liquid–crystalline phase transition of the host phospholipid bilayer is clearly shown by a more gradual, temperature-induced increase in the frequency of the CH_2 symmetric stretching frequency from about 2850 cm^{-1}, which is characteristic of the all-*trans* hydrocarbon chains of gel state phospholipid bilayers, to about 2853 cm^{-1}, which is characteristic of the *gauche* conformer-

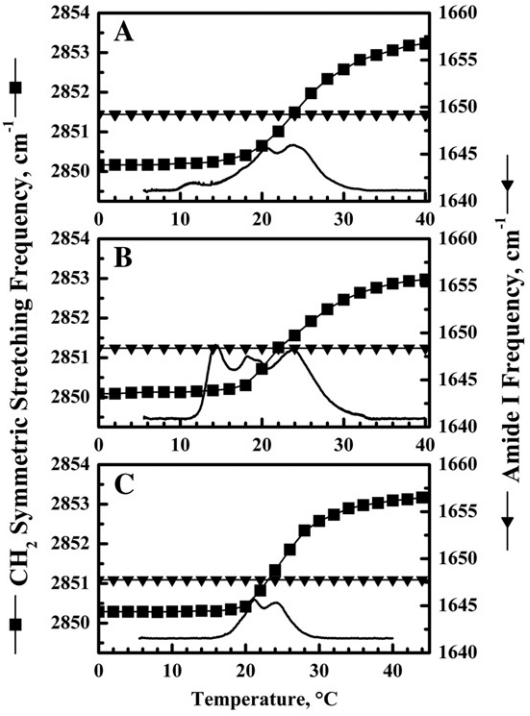

Fig. 11. Representative temperature-dependent changes in the frequencies of the lipid CH_2 symmetric stretching band (–■–) and the peptide amide I band (–▼–) exhibited by peptide-rich samples of DMPC and DMPG. Data are presented for (A) aurein 1.2 in DMPG (30:1), (B) citropin 1.1 in DMPG (30:1), (C) maculatin 1.1 in DMPG (30:1). The DSC heating thermograms exhibited by the samples are shown by the solid line.

containing hydrocarbon chains of liquid–crystalline phospholipid bilayers. Moreover, the temperature range of the phospholipid hydrocarbon chain-melting phase transition as observed by FTIR spectroscopy coincides closely with the higher temperature components of the DSC thermogram, but not with the broad, lowest temperature components (Fig. 11). These observations indicate that neither peptide conformational change nor hydrocarbon chain-melting are involved in the broad lowest-temperature thermotropic event observed in the DSC thermograms exhibited by citropin 1.1-rich mixtures of these peptides with DMPG. However, this may not be true of aurein 1.2- and maculatin 1.1-containing bilayers, where all of the components of the DSC endotherms observed in DMPG vesicles seem to be associated with melting of the phospholipid hydrocarbon chains. Very similar results were observed when each of these peptides were incorporated into DMPC MLVs (data not presented). The nature of the lowest-temperature endothermic event observed by DSC in citropin 1.1-containing DMPC and DMPG vesicles is presently not understood and will require additional study. However, the possibility of significant peptide-induced formation of micelles, small unilamellar vesicles or nonlamellar lipid phases at high peptide concentrations can be eliminated, because ^{31}P-NMR spectroscopic studies performed by us [unpublished data] and others [15,16] indicate that the bilayer structures of the DMPC and DMPG vesicles are maintained even at the highest concentrations of the three frog AMPs used in these studies.

3.3. Inhibition of *A. laidlawii* B growth

The effects of aurein 1.2, citropin 1.1 and maculatin 1.1 on the growth of *A. laidlawii* B, a cell wall-less Gram positive bacterium (Mollicute), were also investigated in order to evaluate the relationship between the results of the physical measurements described above and antimicrobial properties of these peptides. *A. laidlawii* B is well suited for this type of work because the composition, organization and dynamics of its membrane lipid bilayer have been extensively studied [41,42], and because the absence of a cell wall or outer membrane should allow these peptides to interact directly with its cell membrane lipid bilayer, the presumed primary target of this class of AMPs (see [8]). It is generally found that the lipopolysaccharides in the cell wall or outer membrane of Gram-negative bacteria and the lipopeptidoglycan outer layer of Gram-positive bacteria may compete for the binding of AMPs with the lipid bilayer of the inner membrane or physically exclude such peptides from or otherwise impede their access to the periplasmic space [43,44]. Our use of *A. laidlawii* B to assay the antibiotic potencies of these peptides is thus intended to circumvent such problems, so that a clearer relationship may be established between the intrinsic capacities of these peptides to disrupt cell membranes and the calorimetric and spectroscopic data presented here.

The effects of the three peptides on the growth of *A. laidlawii* B are summarized in Table 1. The growth inhibitory activities of aurein 1.2 and citropin 1.1 against *A. laidlawii* B are clearly comparable in magnitude, as evidenced by the similarities in their apparent LD_{50} values (~2.3 μM) and MIC ranges (2.5–5 μM). However, the apparent LD_{50} value obtained for

Table 1
Antimicrobial activity and physicochemical parameters of the antimicrobial peptides aurein 1.2, citropin 1.1 and maculatin 1.1

Peptide properties	Aurein 1.2	Citropin 1.1	Maculatin 1.1
No. of amino acid residues	13	16	21
Molecular weight	1481	1682	2148
Net charge at neutral pH	+1	+2	+3
A. laidlawii B growth inhibition: apparent LD_{50} (μM)	2.31±0.22	2.25±0.18	1.22±0.15
A. laidlawii B growth inhibition: MIC range (μM) [a]	2.5–5.0	2.5–5.0	2.5–5.0
Water to membrane interface partitioning (unfolded) [b]	−0.38	−1.29	0.67
Water to membrane interface partitioning (α-helical) [b]	−5.58	−7.69	−7.73 [c] (−5.8 to −6.0)
Water to octanol partitioning [b]	11.91	10.78	12.11
Helical content (%) [d]	90–95	76–85	65–76
Helical hydrophobic moment [b]	6.77	4.1	6.8 [c] (4.2)

[a] The lowest concentration range within which no growth is detected over a period of 24 h. A MIC range of 2–4 μM indicates that growth is detected at 2 μM but not at 4 μM.

[b] Values (kcal/mol) calculated from the experimentally-determined hydrophobicity scale of White and co-workers [55–57].

[c] Values assume that maculatin 1.1 can be completely α-helical in a lipid membrane. More realistic estimates based on the solution structure of maculatin 1.1 in membrane-mimetic media [5] are given in brackets.

[d] Estimated from analyses of published NMR-determined solution structures of these peptides [4,5,9] in membrane-mimetic solvents.

maculatin 1.1 (~1.2 μM) is lower than that of the other two peptides, indicating that despite the similarities in the observed MIC ranges of these peptides, maculatin is approximately twice as effective at inhibiting *A. laidlawii* B growth. The fact that maculatin 1.1 is more effective at disrupting cell membranes than either aurein 1.2 or citropin 1.1 is consistent with our biophysical data and previously published studies of the interactions of these peptides with model lipid membranes [14–16].

4. Discussion

An important finding of this work is that the magnitude of the effect of the incorporation of the AMPs aurein 1.2, citropin 1.1 and maculatin 1.1 on the thermotropic phase behavior of phospholipid MLVs depends on the structure as well as on the net charge of the phospholipid polar headgroup. Specifically, the incorporation of these peptides has little effect on the temperature, enthalpy or cooperativity of the main phase transition of zwitterionic DMPE bilayers, even after multiple cycling through the gel/liquid–crystalline phase transition temperature. Only after exposure to high temperatures is a small decrease in the temperature, enthalpy and cooperativity of the main phase transition of DMPE MLVs observed. In contrast, the incorporation of these three peptides into zwitterionic DMPC MLVs produces much larger decreases in the temperature, enthalpy and cooperativity of the main phase transition, as well as producing multicomponent DSC endotherms, while their incorporation into anionic DMPG MLVs produces even larger effects on overall thermotropic phase behavior. This underlying pattern of behavior is essentially similar to that noted in similar DSC studies of the interactions of the β-sheet cyclic AMP gramicidin S [22] and several other α-helical AMPs with different phospholipid bilayers (see [45,46]). The fact that the differences between the effects of such peptides on the overall thermotropic phase behavior of the zwitterionic phospholipids DMPE and DMPC are actually larger than between the zwitterionic phospholipid DMPC and the anionic phospholipid DMPG MLVs also indicates that polar headgroup structure can be as important as net polar headgroup charge in determining the strength of the interaction of these peptides with the host phospholipid bilayer.

The observation that aurein 1.2, citropin 1.1 and maculatin 1.1 all interact more strongly with anionic DMPG bilayers than with zwitterionic DMPC and DMPE bilayer is probably due in part to the more favorable electrostatic interactions between these cationic peptides and the negatively charged surfaces of DMPG bilayers. It has been demonstrated that cationic drugs [47] and AMPs [12,13] can disrupt the electrostatic interactions between the positively charged choline (or ethanolamine) moieties and the negatively charged phosphate groups of adjacent phospholipid molecules. Electrostatic attraction between the positively charged residues of these tree frog AMPs and the negatively charged phosphate moieties of the phosphorylcholine and phosphorylethanolamine polar headgroups of DMPC and DMPE is thus highly probable, but when compared with negatively charged lipids such as DMPG, the overall strength of such interaction will be markedly attenuated through competition with the positively charged choline and ethanolamine moieties at the surfaces of DMPC and DMPE bilayers, respectively. Moreover, the strength of such interactions will probably be less pronounced with DMPC bilayers because of steric shielding of the positively charged quaternary nitrogen of the choline moiety by the three attached methyl groups. Because of this, net electrostatic attraction between these peptides and DMPC polar headgroups will probably be stronger than occurs with DMPE bilayers, perhaps accounting in part for the stronger interactions of these peptides with the DMPC as observed in the present study. The idea that electrostatic interactions are an important aspect of the antimicrobial activity and interactions of these peptides with both anionic and zwitterionic bilayers is also consistent with previously published monolayer [14] and infrared spectroscopic [17] studies of these three peptides. Indeed, this seems to be a common feature of most cationic, membrane-targeted AMPs and underscores the functional importance of the positively charged residues of such peptides *in vivo*.

However, other differences between the physical properties of DMPC as DMPE bilayers may also account for the apparently stronger interactions of aurein 1.2, citropin 1.1 and maculatin 1.1 with DMPC compared to DMPE vesicles. For example, these peptides may interact preferentially with liquid–crystalline DMPC rather than DMPE bilayers because of the greater fluidity and decreased packing density of the former phospholipid as compared to the latter (see [34,35]). This suggestion is supported by our present findings that these peptides interact less strongly with gel as compared to liquid–crystalline bilayers of both of these zwitterionic phospholipids and more strongly with DMPC than with DMPE at comparable reduced temperatures in the liquid–crystalline state, and by our observation that significant peptide–DMPE interactions are only observed after exposure to high temperatures. It is also possible that the capacity for hydrogen bond formation between these peptides and the polar headgroup and interfacial regions of the host phospholipid bilayer may also be important in determining the strength and nature of peptide–phospholipid interactions. Similar patterns of behavior were observed in comparable studies of the interaction of the antimicrobial peptide gramicidin S with the polar/apolar interfaces of lipid model membranes and were ascribed to the increased penetration of the polar/apolar interfaces of more disordered lipid bilayers [48]. Additional studies on a wider variety of other lipids will be required to elucidate the nature of these frog antimicrobial-peptide phospholipid interactions in greater detail.

The comparative effects of the incorporation of the frog antimicrobial peptides studied here on the thermotropic phase behavior of zwitterionic and anionic phospholipid bilayers can also be used to deduce both the general location of this peptide relative to the lipid bilayer and the nature of the lipid–peptide interactions involved. For example, Papahadjopoulos et al. [19] and McElhaney [20] have proposed that many membrane-associated proteins can be classified into one of three groups with regard to their interactions with phospholipid bilayers. Group I proteins are typically positively charged, water soluble, peripheral membrane proteins that interact much more strongly with anionic than with zwitterionic lipids. The interactions of

such proteins with anionic phospholipid bilayers typically increase both the temperature and enthalpy of the main phase transition temperature while decreasing its cooperativity only slightly. Group I proteins are localized on the bilayer surface where they interact only with the phospholipid polar headgroups primarily by electrostatic interactions. Group II proteins are also typically positively charged at neutral pH but are somewhat less water soluble and interact somewhat more strongly with anionic than with zwitterionic phospholipid bilayers. The interactions of these proteins with anionic and zwitterionic phospholipid bilayers usually decrease the temperature, enthalpy and cooperativity of the main phase transition moderately, at least at relatively high protein concentrations. Group II proteins are localized at the polar/nonpolar bilayer interface where they interact primarily with the polar headgroups and glycerol backbone region of the phospholipid molecules by both electrostatic and hydrogen bonding interactions, although some hydrophobic interactions with the region of the hydrocarbon chains near the bilayer interface also occurs. Finally, Group III proteins have a range of charges but are water-insoluble, integral membrane proteins that interact equally well with anionic and zwitterionic phospholipid bilayers. The effect of the incorporation of such proteins into phospholipid bilayers is usually to reduce the temperature only slightly but to decrease the enthalpy and cooperativity of the main phase transition markedly. Group III proteins penetrate into or through phospholipid bilayers and interact extensively with the phospholipid hydrocarbon chains by hydrophobic and van der Waal's interactions, as well as with the phospholipid polar headgroups by electrostatic and hydrogen bonding interactions. The incorporation of Group I proteins also usually has little effect on the permeability of the anionic phospholipid vesicles with which they interact, while the incorporation of Group II and Group III proteins increases anionic, and zwitterionic and anionic phospholipid vesicle permeability, respectively. We can conclude from their chemical structures and physical properties, as well as from their effects on the thermotropic phase behavior and permeability of the zwitterionic and anionic phospholipid vesicles, that the three frog AMPs studied here can be classified as Group II proteins. Proteins in this group would thus be expected to reside near the glycerol backbone region of the phospholipid bilayer, with the polar and charged groups of their amphiphilic helices interacting primarily with the polar headgroups of the phospholipid molecules by electrostatic and hydrogen bonding interactions, and with their nonpolar amino acids interacting with the upper regions of the phospholipid hydrocarbon chains via hydrophobic and van der Waal's forces. The location of these peptides in the polar/apolar interfacial regions of zwitterionic and anionic phospholipid bilayers is consistent with the results of our present FTIR spectroscopic studies and with the results of most of the previous studies summarized in Introduction.

As expected, the relative magnitude of the perturbation of the thermotropic phase behavior of each of the phospholipid MLVs investigated here varies considerably with the structure of the frog antimicrobial peptide. Specifically, the relative potencies of these peptides in reducing the temperature, enthalpy and cooperativity of the sharp component, and in altering the temperature and reducing the enthalpy and cooperativity of the broad component of the main phase transition, decrease in the order maculatin 1.1 > aurein 1.2 > citropin 1.1 in both zwitterionic and anionic phospholipid bilayers. These experimental observations are generally compatible with data reported in some NMR spectroscopic studies [16]. For some classes of antimicrobial peptides, variations in their capacity for disrupting lipid bilayers are strongly and positively correlated with variations in the size of the peptide and the net charge carried on their polar surfaces (for examples, see [49–52]). However, although both larger size and greater surface charge may explain why maculatin 1.1 is more disruptive of the structure and organization lipid bilayers than either aurein 1.2 or citropin 1.1, they cannot explain why aurein 1.2 is more effective at disrupting model membranes than citropin 1.1, despite its being smaller than citropin 1.1 and having a lower net charge on its polar surface. Thus, although peptide size and charge are probably significant contributors to the differential capacity of these peptides to perturb the thermotropic phase behavior of phospholipid bilayer membranes, these factors cannot fully explain our experimental findings.

Our data also show that antibiotic potencies of these peptides, as determined by their capacity to inhibit *A. laidlawii* B growth, can be ranked in the following order: maculatin 1.1 > aurein 1.2 ≅ citropin 1.1. This observation is largely compatible with measurements of the relative capacities of these peptides to permeabilize lipid vesicles [53]. The observation that the antibiotic activity of maculatin 1.1 is higher than that of either aurein 1.2 or citropin 1.1 is also compatible with many, though not all, of the assays of the antibiotic activities reported for these peptides (for examples, see [4–6,8]), and with the results of the biophysical studies presented here and elsewhere (see [8,11,14–18]). However, the differences between the antibiotic activities of aurein 1.2 and citropin 1.1 as observed in this and other studies [4–6,8] are not well correlated with our calorimetric data and with other biophysical data reported in the literature [8,11,14–18]. In principle, the higher antibiotic potency of maculatin 1.1 relative to both aurein 1.2 and citropin 1.1 can be rationalized on the basis of its larger size and higher net surface charge. However, as with the calorimetric data discussed above, such considerations cannot explain the small differences between the antibiotic potencies of aurein 1.2 and citropin 1.1 reported here, nor the even wider variations in their relative antibiotic activities that have been reported elsewhere (see [4–6,8]). However, the antibiotic activities determined for membrane-targeted antimicrobial peptides such as these can be strongly influenced by the presence and nature of the bacterial cell wall, which may also influence access to the plasma membrane (see [43,44]), and by the capacity of the organism to degrade the peptide by proteolysis or other means (see [54]). Thus, a strict correlation of *in vivo* assays of antimicrobial activity with the physiochemical properties of AMPs, or with their biophysically-determined propensities for the disruption of phospholipid model membranes, may not always be observed. However, in these studies, cell wall-related issues should not apply to *A. laidlawii* B, the cell wall-less mollicute used to assay antimicrobial activity. Also, because of the strong homology of the amino acid

sequences of aurein 1.2 and citropin 1.1, major differences in their susceptibility to proteolytic degradation under similar conditions is probably unlikely. Consequently, an argument can be made that there should be a better correlation between our assayed antimicrobial activities of aurein 1.2 and citropin 1.1 and their capacity to disrupt lipid bilayers, as determined by the biophysical studies reported here and elsewhere (see [8,11,14–16]). Evidently, there are aspects to the biological activities of these peptides that are not fully captured by biophysical studies of their interactions with lipid model membranes.

Listed in Table 1 are estimates of some selected physicochemical parameters of aurein 1.2, citropin 1.1 and maculatin 1.1, along with the size and charge data alluded to above. The parameters listed therein reveal a number of features which may be relevant to the interpretation of the biological and biophysical data available on these antimicrobial peptides. In particular, we note that the helical hydrophobic moment calculated for aurein 1.2 is greater than that of citropin 1.1, and may even exceed that of maculatin 1.1, once the latter is appropriately weighted for the helix-destabilizing effect of its Pro-15 residue. This implies that aurein 1.2 is inherently the most amphipathic of the three peptides studied, and suggests that despite its smaller size, aurein 1.2 helices may have a stronger affinity for hydrophobic surfaces and lipid membranes than those of citropin 1.1. This suggestion is supported by studies showing that aurein 1.2 is more strongly retained by reversed phase HPLC columns than citropin 1.1 (unpublished experiments from this laboratory). The large positive values for the water-to-octanol partitioning free energies (10–12 kcal/mol) also suggest that partitioning of all three peptides into the hydrophobic domains of lipid membranes should be highly unfavorable relative to their partitioning into the aqueous phase. In contrast, the sizeable negative values (−5 to −8 kcal/mol) calculated for the transfer of α-helical conformers of these peptides into membrane polar/apolar interfaces from water suggests that that process should be highly favorable, although the same is not the case for the transfer of the unstructured conformers of these peptides into membrane polar apolar interfaces from water (partitioning free energies −0.4 to −1.3 kcal/mol). In this respect, the calculated partitioning free energies are consistent with the sizeable body of experimental evidence indicating that these peptides have a high propensity for partitioning into membrane polar/apolar interfaces as α-helices [this work, 15,16]. Interestingly, the data shown also suggest that the transfer of aurein 1.2 helices into membrane interfaces (−5.8 kcal/mol) should be less favorable than the corresponding transfer of citropin 1.1 and maculatin 1.1 helices by ∼2 kcal/mol. However, these helix partitioning free energy values are based on the assumption that the peptides are completely helical when partitioned into the polar apolar interfaces of lipid membranes. NMR solution structure studies of these peptides [3–5,9] indicate that although such an assumption is tenable with aurein 1.2 and citropin 1.1, it cannot hold with maculatin 1.1, mainly because of the helix disruption caused by the Pro-15 residue. Thus, when weighted for the helix-disrupting effects of the Pro-15 residue, the estimates of the free energy of transferring maculatin 1.1 from water to membrane interfaces become less favorable by about 1.8 to 2 kcal/mol (see Table 1). This observation illustrates clearly that the water-to-membrane partitioning properties of peptides such as these are quite sensitive to their overall α-helical-forming propensities, the effects of which are not usually considered in studies such as these.

We also note that aside from the differences in size, the major significant differences between aurein 1.2 and citropin 1.1 are the valine substitutions at Ile-5, Ile-9 and Ser-12 of aurein 1.2, and a serine substitution at Glu-11. However, because of the lower helix-forming propensity of valine (see [58,59]), and the fact that the mean helix-forming propensity of the extension GGL sequence at the C-terminus of citropin 1.1 is also relatively low, α-helical structures formed by citropin 1.1 will probably be less stable than those formed by aurein 1.2. Also, the α-helices formed by aurein 1.2 will probably be further stabilized by $i+3$ and $i+4$ salt bridge interactions between the negatively charged Glu-11 side chains and the positively charged amino side chains at Lys-7 and Lys-8, in marked contrast to the citropin 1.1 α-helices, for which such interactions are precluded by the Glu-11 to Ser-11 substitution. With maculatin 1.1, one can also argue that because of the combined helix-destabilizing effects of its four valine residues and Pro-15 residue, along with the fact there is no potential for helix stabilization by $i+3$ and $i+4$ ionic interactions between side chains, this peptide will probably form α-helices that are less stable than those formed by aurein 1.2 or possibly even citropin 1.1. Such arguments are supported by our analyses of previously published NMR-determined solution structures of these peptides in membrane-mimetic solvents (see [4,5,9]), which indicate that the helical content of conformers formed under such conditions differ significantly and decrease in the order aurein 1.2 > citropin 1.1 > maculatin 1.1 (see Table 1). We therefore suggest that because of its higher α-helical-forming propensity and tendency to fold into more stable α-helices, the partitioning of aurein 1.2 into the polar/apolar interfaces of lipid membranes will probably be more favorable than suggested by the partitioning free energy estimates listed in Table 1, which assume complete and comparable helical conformations. Moreover, this effect, along with its higher helical hydrophobic moment (see Table 1), may even make aurein 1.2 more prone to partition into the polar/apolar interfaces of lipid membranes than either citropin 1.1 or maculatin 1.1.

In principle, the suggestion that aurein 1.2 may actually be more prone to partition into membrane polar/apolar interfaces than either citropin 1.1 or maculatin 1.1, in combination with effects attributable to differences in the size and net charges of these peptides, can provide a plausible framework for rationalizing our experimental observations. Given its larger size and greater net charge on its polar surface, maculatin 1.1 will be inherently more disruptive of the structure and organization of lipid membranes per mol bound than either citropin 1.1 or aurein 1.2. Although these membrane-disruptive properties will be attenuated by its overall lower propensity for partitioning into lipid membranes, the magnitude of the size and charge differential between maculatin 1.1 and the other peptides (especially aurein 1.2) is such that size and charge-related effects are likely to predominate, as long as the differences between the

partitioning of the peptides are not excessive. However, with aurein 1.2 and citropin 1.1, the size and charge differential between the two peptides is considerably smaller and as a result, effects attributable to the higher membrane partitioning propensity of aurein 1.2 will probably be more noticeable. We therefore suggest that these effects are likely manifested by the greater disruption of model lipid membranes by aurein 1.2 as noted in these and other biophysical studies, and in the small differences between the assayed antimicrobial activities of these two peptides. An evaluation of the relationship between the partitioning of these peptides into various lipid membranes and their capacity for disrupting both model and biological membranes is at the focus of our ongoing investigations.

Acknowledgments

Supported by an Operating Grant from the Canadian Institutes for Health Research (RNM), Major Equipment Grants from the Alberta Heritage Foundation for Medical Research (RNM), an Operating Grant from the Australian Research Council (FS), and by Summer Research Studentships from the Alberta Heritage Foundation for Medical Research (GWJS and SM) and the Natural Sciences and Engineering Research Council of Canada (DWK).

References

[1] L.H. Lazarus, M. Attil, The toad, ugly and venomous, wears yet a precious jewel in his skin, Prog. Neurobiol. 41 (1993) 473–507.
[2] M.A. Apponyi, T.L. Pukala, C.S. Brindworth, V.M. Maselli, J.H. Bowie, M.J. Tyler, G.W. Booker, J.C. Wallace, J.A. Carver, F. Separovic, J. Doyle, L.E. Llewellyn, Host-defense peptides of Australian anurans: structure, mechanism of action and evolutionary significance, Peptides 25 (2004) 1035–1054.
[3] T.K. Rozek, L. Wegener, J.H. Bowie, I.N. Olver, J.A. Carver, J.C. Wallace, M.J. Tyler, The antibiotic and anticancer active aurein peptides from the Australian Bell Frogs *Litoria aurea* and *Litoria raniformis*. The solution structure of aurein 1.2, Eur. J. Biochem. 267 (2000) 5330–5341.
[4] K.L. Wegener, P.A. Wabnitz, J.A. Carver, J.H. Bowie, B.C.S. Chia, J.C. Wallace, M.J. Tyler, Host defense peptides from the skin glands of the Australian Blue Mountains tree frog *Litoria citropa*. Solution structure of the antibacterial peptide citropin 1.1, Eur. J. Biochem. 265 (1999) 627–637.
[5] B.C.S. Chia, J.A. Carver, T.D. Mulhern, J.H. Bowie, Maculatin 1.1, an antimicrobial peptide from the Australian tree frog, *Litoria genimaculata*. Solution structure and biological activity, Eur. J. Biochem. 267 (2000) 1894–1908.
[6] T. Rozek, J.H. Bowie, J.C. Wallace, M.J. Tyler, The antibiotic and anticancer active aurein peptides from the Australian bell frogs *Litoria aurea* and *Litoria raniformis*. Part 2. Sequence determination using electronspray mass spectrometry, Rapid Commun. Mass Spectrom. 14 (2000) 2002–2011.
[7] S.E. Van Compermolle, R.J. Taylor, K. Oswald-Richter, J. Jiang, B.E. Youree, M.J. Tyler, J.M. Conlon, D. Wade, C. Aiken, T.S. Dermody, V.N. Kewal Ramani, L.A. Rollins-Smith, D. Unutmaz, Antimicrobial peptides from amphibian skin potently inhibit human immunodeficiency virus infection and transfer of virus from dendritic cells to T cells, J. Virol. 79 (2005) 11598–11606.
[8] M.P. Boland, F. Separovic, Membrane interactions of antimicrobial peptides from Australian tree frogs, Biochim. Biophys. Acta 1758 (2006) 1178–1183.
[9] G. Wang, Y. Li, X. Li, Correlation of three-dimensional structures with the antibacterial activity of a group of peptides designed based on a nontoxic bacterial membrane anchor, J. Biol. Chem. 280 (2005) 5803–5811.
[10] H. Wong, J.H. Bowie, J.A. Carver, The solution structure and activity of caerin 1.1, an antimicrobial peptide from the Australian green tree frog, *Litoria splendida*, Eur. J. Biochem. 247 (1997) 545–557.
[11] T.K. Niidome, K. Kobayashi, H. Arakawa, T. Hatakeyama, H. Aoyagi, Structure–activity relationship of an antibacterial peptide, maculatin 1.1, from the skin glands of the tree frog, *Litoria genimaculata*, J. Pept. Sci. 10 (2004) 414–422.
[12] U.H.N. Durr, U.S. Sudheendra, A. Ramamoorty, LL-37, the only human member of the cathelicidin family of antimicrobial peptides, Biochim. Biophys. Acta 1758 (2006) 1393–1407.
[13] B.K. Bechinger, K. Lohner, Detergent-like actions of linear amphiphilic cationic antimicrobial peptides, Biochim. Biophys. Acta 1758 (2006) 1529–1539.
[14] E.E. Ambroggio, F. Separovic, J.H. Bowie, G.D. Fidelio, Surface behaviour and peptide–lipid interactions of the antibiotic peptides, maculatin and citropin, Biochim. Biophys. Acta 1664 (2004) 31–37.
[15] M.S. Balla, J.H. Bowie, F. Separovic, Solid-state NMR study of antimicrobial peptides from Australian frogs in phospholipid membranes, Eur. Biophys. J. 33 (2004) 109–116.
[16] I. Marcotte, K.L. Wenger, Y.-H. Lam, B.C.S. Chia, M.R.R. de Planque, J.H. Bowie, M. Auger, F. Separovic, Interaction of antimicrobial peptides from Australian amphibians with lipid membranes, Chem. Phys. Lipids 122 (2003) 107–120.
[17] C.S.B. Chia, J. Torres, M.A. Cooper, I.T. Arkin, J.H. Bowie, The orientation of the antibiotic peptide maculatin 1.1 in DMPG and DMPC bilayers. Support for a pore-forming mechanism, FEBS Lett. 512 (2002) 47–51.
[18] B.C.S. Chia, Y.-H. Lam, M. Dyall-Smith, F. Separovic, J.H. Bowie, A ^{31}P NMR study of the interaction of amphibian antimicrobial peptides with the membranes of live bacteria, Lett. Pept. Sci. 7 (2000) 151–156.
[19] D. Papahadjoupolos, M. Moscarello, E.H. Eylar, T. Issac, Effects of proteins on thermotropic phase transitions of phospholipid membranes, Biochim. Biophys. Acta 401 (1975) 317–335.
[20] R.N. McElhaney, The use of differential scanning calorimetry and differential thermal analysis in studies of model and biological membranes, Chem. Phys. Lipids 30 (1982) 229–259.
[21] R.N. McElhaney, Differential scanning calorimetric studies of lipid–protein interactions in model membrane systems, Biochim. Biophys. Acta 864 (1986) 361–421.
[22] E.J. Prenner, R.N.A.H. Lewis, L.H. Kondejewski, R.S. Hodges, R.N. McElhaney, Differential scanning calorimetric study of the effect of the antimicrobial peptide gramicidin S on the thermotropic phase behaviour of phosphatidylcholine, phosphatidylethanolamine and phosphatidylglycerol lipid bilayer membranes, Biochim. Biophys. Acta 1417 (1999) 211–223.
[23] K. Lohner, E.J. Prenner, Differential scanning and X-ray diffraction studies of the specificity of the interaction of antimicrobial peptides with membrane-mimetic systems, Biochim. Biophys. Acta 1462 (1999) 141–156.
[24] R.N. Merrified, Solid phase peptide synthesis. 1. The synthesis of a tetrapeptide, J. Am. Chem. Soc. 85 (1963) 2149–2154.
[25] N.J. Maeji, A.M. Bray, R.M. Valerio, W. Wang, Larger scale multipin peptide synthesis, Pept. Res. 8 (1995) 33–38.
[26] R.N.A.H. Lewis, Y.-P. Zhang, R.N. McElhaney, Calorimetric and spectroscopic studies of the phase behaviour and organization of lipid bilayer model membranes composed of binary mixtures of dimyristoylphosphatidylcholine and dimyristolyphosphatidylglycerol, Biochim. Biophys. Acta 168 (2005) 203–214.
[27] H.H. Mantsch, C. Madec, R.N.A.H. Lewis, R.N. McElhaney, Thermotropic phase behavior of model membranes composed of phosphatidylcholines containing iso-branched fatty acids. 2. Infrared and ^{31}P-NMR spectroscopic studies, Biochemistry 24 (1985) 2440–2446.
[28] J.R. Silvius, R.N. McElhaney, Lipid compositional manipulation in *Acholeplasma laidlawii* B. Effect on exogenous fatty acids on fatty acid composition and cell growth when endogenous fatty acid production is inhibited, Can. J. Biochem. 56 (1978) 462–469.
[29] E.J. Prenner, M. Kiricsi, M. Jelokhani-Niaraki, R.N.A.H. Lewis, R.S.

Hodges, N. McElhaney, Structure–activity relationships of diastereomeric lysine ring-size analogs of the antimicrobial peptide gramicidin S: mechanism of action and discrimination between bacterial and animal cell membranes, J. Biol. Chem. 280 (2005) 2002–2011.

[30] R.N.A.H. Lewis, N. Mak, R.N. McElhaney, A differential scanning calorimetric study of the thermotropic phase behaviour of model membranes composed of phosphatidylcholines containing linear saturated fatty acyl chains, Biochemistry 26 (1987) 6118–6126.

[31] Y.-P. Zhang, R.N.A.H. Lewis, R.S. Hodges, R.N. McElhaney, Interactions of a peptide model of a hydrophobic transmembrane α-helical segment of a membrane protein with phosphatidylcholine bilayers: differential scanning calorimetric and FTIR spectroscopic studies, Biochemistry 31 (1992) 11579–11588.

[32] Y.-P. Zhang, R.N.A.H. Lewis, R.S. Hodges, R.N. McElhaney, Peptide models of helical hydrophobic transmembrane segments of membrane proteins. II. DSC and FTIR spectroscopic studies of the interaction of A_C-K_2-$(LA)_{12}$-K_2-amide with phosphatidylcholine bilayers, Biochemistry 34 (1995) 2362–2371.

[33] Y.-P. Zhang, R.N.A.H. Lewis, R.N. McElhaney, Calorimetric and spectroscopic studies of the thermotropic phase behavior of the *n*-saturated 1,2-diacylphosphatidylglycerols, Biophys. J. 72 (1997) 779–793.

[34] R.N.A.H. Lewis, R.N. McElhaney, Calorimetric and thermotropic studies of the polymorphic phase behaviour of a homologous series of *n*-saturated 1,2-diacylphosphatidylethanolamines, Biophys. J. 64 (1993) 1081–1096.

[35] H. Yao, I. Hatta, R. Koynova, B. Tenchov, Time-resolved X-ray diffraction and calorimetric studies at low scan rates II. On the fine structure of the phase transition of hydrated dipalmitoyl phosphatidylethanolamine, Biophys. J. 61 (1992) 683–693.

[36] L.K. Tamm, S.A. Tatulian, Infrared spectroscopy of proteins and peptides in lipid bilayers, Q. Rev. Biophysics 30 (1997) 365–429.

[37] Y.-P. Zhang, R.N.A.H. Lewis, R.S. Hodges, R.N. McElhaney, FTIR spectroscopic studies of the conformation and amide hydrogen exchange of a peptide model of the hydrophobic transmembrane α-helices of membrane proteins, Biochemistry 31 (1992) 11572–11578.

[38] Y.-P. Zhang, R.N.A.H. Lewis, G.D. Henry, B.D. Sykes, R.S. Hodges, R.N. McElhaney, Peptide models of helical hydrophobic segments of membrane proteins. I. Studies of the conformation, intrabilayer orientation and amide hydrogen exchangeability of A_C-K_2-$(LA)_{12}$-K_2-amide, Biochemistry 34 (1995) 2348–2361.

[39] R.N.A.H. Lewis, R.N. McElhaney, FTIR spectroscopy in the study of hydrated lipids and lipid bilayer membranes, in: H.H. Mantsch, D. Chapman (Eds.), Infrared Spectroscopy of Biomolecules, John Wiley & Sons, N.Y., 1996, pp. 159–202.

[40] R.N.A.H. Lewis, R.N. McElhaney, Vibrational spectroscopy of lipids, in: J.M. Chalmers, P.R. Griffith (Eds.), Handbook of Vibrational Spectroscopy, vol. 5, John Wiley and Sons, Chichester, England, 2002, pp. 3447–3464.

[41] P.F. Smith, Membrane lipid and lipopolysaccharide structures, in: J. Maniloff, R.N. McElhaney, L.R. Finch, J.B. Baseman (Eds.), Mycoplasmas: Molecular Biology and Pathogenesis, American Society for Microbiology, Washington, D.C., 1992, pp. 79–91.

[42] R.N. McElhaney, Membrane structure, in: L. Maniloff, R.N. McElhaney, L.R. Finch, J.B. Baseman (Eds.), Mycoplasmas: Molecular Biology and Pathogenesis, American Society for Microbiology, Washington, D.C., 1992, pp. 113–155.

[43] L.H. Kondejewski, S.W. Farmer, D.S. Wishart, C.M. Kay, R.E.W. Hancock, R.S. Hodges, Modulation of structure and antibacterial and haemolytic activity by ring size cyclic gramicidin s analogs, J. Biol. Chem. 271 (1996) 25261–25268.

[44] M. Kiricsi, E.J. Prenner, M. Jelokhani-Niaraki, R.N.A.H. Lewis, R.S. Hodges, R.N. McElhaney, The effects of ring-size analogs of the antimicrobial peptide gramicidin S on phospholipid bilayer model membranes and on the growth of *Acholeplasma laidlawii* B, Eur. J. Biochem. 269 (2002) 5911–5920.

[45] K.A. Henzler-Wildman, G.V. Martinez, M.F. Brown, A. Ranamoorthy, Perturbation of the hydrophobic core of lipid bilayers by the human antimicrobial peptide LL-37, Biochemistry 43 (2004) 8459–8469.

[46] A. Ramamoorthy, S. Thennarasu, D.-K. Lee, A. Tan, L. Maloy, Solid-state NMR investigation of the membrane-disrupting mechanism of antimicrobial peptides MSI-78 and MSI-594 derived from magainin 2 and mellitin, Biophys. J. 91 (2006) 206–216.

[47] J.S. Santos, D.-K. Lee, A. Ramamoorthy, Effects of antidepressants on the conformation of phospholipid headgroups studied by solid-state NMR, Magn. Reson. Chem. 42 (2004) 105–114.

[48] R.N.A.H. Lewis, E.J. Prenner, L.H. Kondejewski, C.R. Flach, R. Mendelsohn, R.S. Hodges, R.N. McElhaney, Fourier transform infrared spectroscopic studies of the interaction of the antimicrobial peptide gramicidin S with lipid micelles and with lipid monolayer and bilayer membranes, Biochemistry 38 (1999) 15193–15203.

[49] A. Giangaspero, L. Sandri, A. Tossi, Amphipathic α helical antimicrobial peptides. A systematic study of the effects of structural and physical properties on biological activity, Eur. J. Biochem. 268 (2001) 5589–5600.

[50] T. Niidome, N. Matsuyama, M. Kunihara, T. Hatakeyama, H. Aoyagi, Effect of chain length model peptides on antibacterial activity, Bull. Chem. Soc. Jpn. 78 (2005) 473–476.

[51] N. Ohmori, T. Niidome, T. Hatakeyama, H. Mihara, H. Aoyagi, Interaction of alpha-helical peptides with phospholipid model membranes: effects of chain length and hydrophobicity of peptides, J. Pept. Res. 51 (1998) 103–109.

[52] L. Beven, S. Castano, J. Duforcq, A. Wieslander, H. Wroblewski, Yhe antibiotic activity of cationic linear amphipathic peptides: lessons from the action of leucine/lysine copolymers on bacteria of he class Mollicutes, Eur. J. Biochem. 270 (2003) 2207–2217.

[53] E.E. Ambroggio, F. Separovic, J.H. Bowie, G.D. Fidelio, L.A. Bagotolli, Direct visualization of membrane leakage induced by the antibiotic peptides: maculatin, citropin and aurein, Biophys. J. 89 (2005) 1874–1881.

[54] Y. Chen, A.I. Vasil, L. Rehaume, C.T. Mant, J.L. Burns, M.L. Vasil, R.E.W. Hancock, R.S. Hodges, Comparison of biophysical and biologic properties of α-helical enantiomeric antimicrobial peptides, Chem. Biol. Drug Des. 67 (2006) 162–173.

[55] W.C. Wimley, S.H. White, Experimentally determined hydrophobicity scale for proteins at membrane interfaces, Nat. Struct. Biol. 3 (1996) 842–848.

[56] W.C. Wimley, T.P. Creamer, S.H. White, Solvation energies of amino acid side chains and backbone in a family of host guest pentapeptides, Biochemistry 35 (1996) 5109–5124.

[57] S.H. White, W.C. Wimley, Membrane protein folding and stability: physical principles, Annu. Rev. Biophys. Biomol. Struct. 28 (1999) 319–365.

[58] M. Blaber, X. Zhang, B.W. Mathews, Structural basis of amino acid α-helix propensity, Science 260 (1993) 1637–1640.

[59] C.N. Pace, J.M. Scholtz, A helix propensity scale based on experimental studies of peptides and proteins, Biophys. J. 75 (1998) 422–427.